ADVANCING EARTH AND SPACE SCIENCES

JGR Oceans

RESEARCH ARTICLE

10.1029/2024JC022001

Key Points:

- The cold anomaly is quantified as marine cold spells and Fresh Waves cycling between cool/fresh and warm/saline conditions since 1980s
- The 2014–16 cold anomaly, a widespread and prolonged event, increased productivity and oxygenation but intensified ocean acidification
- The cold anomaly contrasts with the Pacific's warm blob with opposite physical and biogeochemical impacts, possibly aiding marine species

Supporting Information:

Supporting Information may be found in the online version of this article.

Correspondence to:

F. Jebri,
fatma.jebri@noc.ac.uk

Citation:

Jebri, F., Jacobs, Z. L., Srokosz, M., Popova, E., Hartman, S. E., & Josey, S. A. (2025). Cold spells, fresh waves, and the biogeochemical response in the North Atlantic cold anomaly region. *Journal of Geophysical Research: Oceans*, *130*, e2024JC022001. https://doi.org/10.1029/2024JC022001

Received 18 OCT 2024
Accepted 24 MAR 2025

Author Contributions:

Conceptualization: Fatma Jebri, Meric Srokosz
Data curation: Fatma Jebri, Zoe L. Jacobs, Susan E. Hartman
Formal analysis: Fatma Jebri, Zoe L. Jacobs
Funding acquisition: Fatma Jebri, Zoe L. Jacobs, Ekaterina Popova
Methodology: Fatma Jebri, Zoe L. Jacobs, Meric Srokosz, Ekaterina Popova
Validation: Simon A. Josey
Writing – original draft: Fatma Jebri
Writing – review & editing: Fatma Jebri, Zoe L. Jacobs, Meric Srokosz, Ekaterina Popova, Susan E. Hartman, Simon A. Josey

Cold Spells, Fresh Waves, and the Biogeochemical Response in the North Atlantic Cold Anomaly Region

Fatma Jebri[1], Zoe L. Jacobs[1], Meric Srokosz[1], Ekaterina Popova[1], Susan E. Hartman[1], and Simon A. Josey[1]

[1]National Oceanography Centre, Southampton, UK

Abstract Regional effects of marine cold spells (MCS, periods of anomalous cooling), their impact on ecosystem biogeochemistry, and link to salinity extremes remain underexplored. A case in point is North Atlantic's Cold Anomaly (CA) region (known as the "cold blob"), which hits record low temperatures during 2014–16 while most of the global ocean warmed. Using up to 42 years of observations, we characterize the CA as a manifestation of both MCS and Fresh Waves (FW, low salinity extremes) and analyze the surface biogeochemical response. We observe a quasiperiodic pattern of MCS from the 1980s and FW (at least) from the 1990s to early 2020s in the CA region with alternations from cool and freshwater to warm and saline conditions. Since 1990s, the CA region appears to be potentially undergoing MCS and FW compound events that are more frequent and prolonged but less intense than other North Atlantic areas. The 2014-16 CA was among the most widespread and prolonged MCS and FW events associated with a deeper mixed layer and distinct biogeochemical signature, including elevated nutrients and oxygen, an overall increased chlorophyll-a and intensified ocean acidification. These results suggest that MCS could mitigate certain climate change effects through cooling and enhanced productivity, while exacerbating others such as ocean acidification. We compare 2014–16 CA region effects with those of Pacific's warm blob, identifying contrasting behaviors from physical processes to biogeochemical impacts and discussing a common atmospheric driver. Our findings emphasize the need to further study ecological responses to MCS in the North Atlantic.

Plain Language Summary Marine cold spells (MCS) are periods of unusual ocean cooling, but their regional effects on ecosystems and links to changes in salinity are not well understood. One example is North Atlantic "cold blob" region, which saw record low temperatures from 2014 to 2016, whereas most oceans experienced pervasive warming. Over 40 years of observations reveal that the cold blob manifests as both MCS and low-salinity events called Fresh Waves (FW). The observations show a pattern of alternating cool, fresh and warm, salty water between 1980s and early 2020s. Since the 1990s, MCS and FW in the cold blob region have become more frequent and last longer but are less intense than in other areas of the North Atlantic. The 2014–2016 cold blob was a major event, leading to changes in ocean conditions, including deeper mixing of water, increased nutrients, higher chlorophyll-a, and more oxygenation and ocean acidification. This suggests that although MCS may help reduce some effects of climate change by cooling waters and boosting productivity, they could also worsen acidification. We highlight the cold blob and Pacific's warm blob contrasting impacts on physical and biogeochemical processes. Understanding marine extremes in the North Atlantic continues to be a challenging problem.

1. Introduction

Recent years witnessed a significant rise in extreme temperature events that are becoming more common with global warming and a changing climate. Hence, there has been a growing focus on marine heat waves (MHW), their drivers and impacts (e.g., Holbrook et al., 2019). The counterpart of MHW, marine cold spells (MCS, prolonged periods of extremely cold ocean temperatures) have not garnered as much research interest. Schelgel et al. (2021) reviewed our understanding of MCS globally and presented a method to define these extreme cooling events based on Hobday et al. (2016) approach in which sea surface temperature (SST) falls below the 10th percentile for at least 5 days relative to a baseline period typically of 30 years. Other studies compared global MHW and MCS concomitant changes and their trends (Peal et al., 2023; Wang et al., 2022), concluding that MHW are increasing in frequency and intensity whereas MCS are diminishing in intensity, frequency, and annual days over the last decades. It has been established that MHW can have significant regional impacts on marine ecosystems and their services (i.e., benefits provided to humans), weather, and socioeconomics. However, MCS

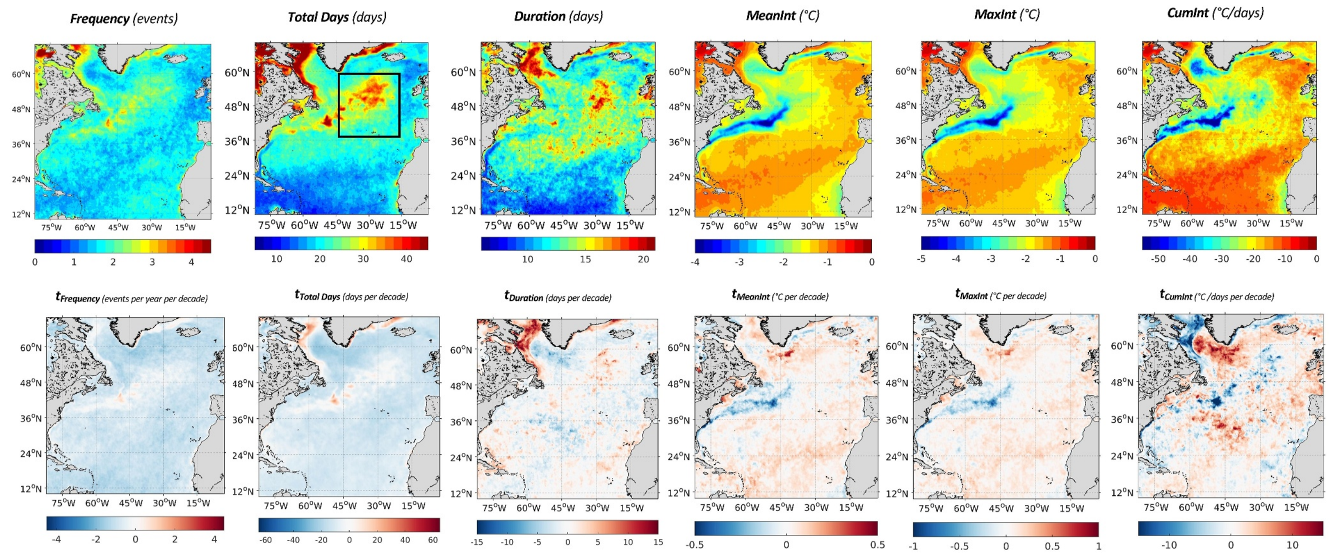

Figure 1. MCS metrics top mean states and bottom trends during 1982–2023. "*t*" indicates trend. To avoid showing very low values, decadal trends are plotted instead of annual ones.

regional effects in terms of characteristics and resulting changes in marine ecosystem biogeochemistry are less investigated with key knowledge gaps in several regions despite some robust efforts—mainly in coastal regions (Cetina-Heredia & Allende-Arandía, 2023; Lubitz et al., 2024; Mohamed et al., 2023; Reyes-Mendoza et al., 2022; Schlegel et al., 2017, 2021). It is also unclear how MCS co-occurring with compound biogeochemical events (which can amplify the effects on the marine ecosystem) are acting regionally. MCS can result in a multitude of ecological impacts and can disturb biogeochemical cycling. These impacts were widely documented in different areas around the global ocean (Schlegel et al., 2021 and references therein). For example, widespread mortality of species (e.g., off Florida in 2010, Collela et al., 2012), population decrease (Zapata et al., 2011), growth phenology (Jentsch et al., 2007), elevated nutrients levels with excessive phytoplankton biomass leading to hypoxic conditions (e.g., California coast in 2002, Wheeler et al., 2003) or eutrophication have all been reported. How severe MCS biogeochemical impacts can get is dependent on both species' tolerance to these extremes MCS characteristics such as their spatial coverage, time of occurrence, duration, and intensity (Grant et al., 2017; Schlegel et al., 2021). MCS could also sometimes lead to ecological benefits such as offering a thermal refugia or recovery period to marine species from extreme warming (Dalsin et al., 2023; Feng et al., 2020). Thus, identifying MCS regions that are more likely to have a favorable influence on the marine ecosystem can allow for better management and planning strategies.

Generally, few studies have investigated MCS in the North Atlantic (e.g., Jacobs et al., 2024) and less so for the Cold Anomaly (CA) region (see box in Figure 1 for the location of this region) (commonly referred to as the "cold blob") in North Atlantic mid to high latitudes that was especially prominent between 2014 and 16 (e.g., Josey et al., 2018). Note that, hereafter, "CA region" indicates a North Atlantic region that witnesses a number of cold events, one of the strongest was observed in 2014–16 and that this CA region is not to be confused with a single specific event. The anomalous cooling (by ∼1–2°C) in 2014–16 captured world-wide attention as a transient feature. The location of this anomalous cooling is similar to the North Atlantic "warming hole" that occurred in annual trends of SST since 1901 with values down to 0.9°C below normal, whereas the rest of the global temperature rise reached >1°C (Henson, 2016; Rahmstorf et al., 2015). Several studies examined the CA region's physical drivers and consequences on weather (e.g., Henson, 2016; Josey et al., 2018; Robson et al., 2016), including occurrences prior to 2014–16 and as far back as the 1950s (e.g., Liang et al., 2017; Shi et al., 2023). The main mechanism behind the cold anomaly during 2015 is an intense surface heat loss due to variations in atmospheric circulation in the winter of 2014–15 coupled with an intense heat loss in preceding winter of 2013–14 that formed the re-emergence of a cold water anomaly (Duchez et al., 2016). About 70% of the re-emergence during the second half of 2014 was found due to vertical diffusion (Sanders et al., 2022), which constitutes another mechanism behind this re-emergence. The exceptional air-sea heat loss in 2013–14 winter was associated with a dominant positive Eastern Atlantic Pattern (EAP) and followed by a prevailing positive phase of the North Atlantic Oscillation (NAO) in 2014–15 winter (Josey et al., 2018; Sanders et al., 2022; Yeager et al., 2016). The 2015 cool temperatures were linked to reduced summer surface warming of the mixed layer (Sanders et al., 2022). A slowdown in the Atlantic Meridional Overturning Circulation (AMOC) can also directly affect part of the CA region leading to cooling as shown by Bryden et al. (2014, their Figure 7) especially if the changes are large. Furthermore, model results lend support to the hypothesis that a potential externally forced decline in the AMOC since the mid-1990s can precondition the subpolar North Atlantic, and so the CA region, allowing record lows to occur via processes involving internal climate variability such as the NAO (Schlegal et al., 2021; Yeager et al., 2016). The CA region in 2014–16 is thought to influence European climate through impacts on the NAO and terrestrial heat waves (Josey et al., 2018).

The cold blob phenomenon has also been catching the press's attention with numerous newspaper articles as recent as late 2023 (e.g., Mooney, 2015; Ramirez Grand, 2023). Unlike the Pacific blob, which has been extensively studied as an MHW from physics (e.g., Di Lorenzo & Mantua, 2016) to biogeochemistry (Mogen et al., 2022) and ecosystem impacts (e.g., Suryan et al., 2021), the Atlantic cold blob has not been examined as a manifestation of MCS using the Hobday et al. (2016) framework (which objectively characterizes extreme temperature events), although it was studied as a region where unusually cool temperatures occurred (e.g., Duchez et al., 2016; Josey et al., 2018; Shi et al., 2023). The only exception is an application by Schlegel et al. (2021) that briefly looked at MCS 2013–2016 event over the CA region focusing only on a specific location (a focal point) rather than the wider CA region and without a complete assessment of MCS metrics (such as the frequency, total days and mean intensity). Additionally, studies have yet to link MCS to salinity extremes in the CA region as compound extreme events can have greater effects, although some research suggested possible connections between the blob cooling and subpolar North Atlantic exceptional freshening during 2014–16 and the Great Salinity Anomaly (GSA) in the 80 and 90s (Biló et al., 2022; Holiday et al., 2020). More importantly, the biogeochemical response of the CA region in 2014–16 remains unknown, and addressing it could be key to understanding the ecosystem impacts of this exceptional cooling in the North Atlantic.

Here, we investigate MCS, Fresh Waves (FW, low salinity extremes) in the North Atlantic, and the surface biogeochemical response over the CA region for the past 26–42 years using Earth Observation data. Note that our emphasis is on the upper layer (0–10 m) as extremes at the surface like in temperature, salinity, and oxygen significantly impact marine ecosystems, including fish species and biodiversity (Brauko et al., 2020; Li et al., 2024; Liu et al., 2023; Mattiasen et al., 2020). We highlight the contrasting behavior between the effects of Atlantic CA region in 2014–16 and Pacific warm blob, which occurred at the same time period, and discuss potential ecological implications.

2. Materials and Methods

2.1. Earth Observations

Daily and gap-free satellite-derived sea surface temperature (SST) and Chlorophyll-a (Chl-a) from global reprocessed products are used. The SST data are available on a 0.05° spatial resolution from the multisatellite Operational Sea Surface Temperature and Sea Ice Analysis (OSTIA) product that we download from Copernicus Marine Environment Monitoring Service (CMEMS) (http://marine.copernicus.eu/services-portfolio/access-to-products/) over the period 1982–2023. The Chl-a ocean color product is from the GlobColour project (http://globcolour.info) with a 4 km resolution retrieved from CMEMS (http://marine.copernicus.eu/services-portfolio/access-to-products/) from 1998 to 2022. Satellite observations have some known limitations such as the overestimation of Chl-a values near the coasts and in shallow optically complex waters (generally <30 m, Zhang et al., 2006). This is because of the bottom reflectance issues and suspended material (dissolved organic matter and suspended material), which can lead to elevated water-leaving radiance, hence exaggerating Chl-a correction term (IOCCG, 2000). Nonetheless, the CA region is in the open ocean comprising Case-1 waters (i.e., where concentration of phytoplankton is high compared to other particles) deeper than 200 m.

We use surface oxygen and nutrients ($NO_2 + NO_3$) from World Ocean Database 2018 (WOD18, Boyer et al., 2018) for individual measurements between 2014 and 2016 over the CA box (Figure S1 in Supporting Information S1). These are compared with the corresponding climatological values (1965–2022) from the World Ocean Atlas 2023 (WOA23, Garcia, Wang, et al., 2024; Garcia, Bouchard, et al., 2024). WOA23 includes objectively analyzed and quality-controlled fields from all available observations in the WOD, namely ocean stations, Moored buoys, ship-based CTDs, and profiling floats over the CA region. Note that WOD18 and WOA23 are the most updated versions of the WOD and WOA data and that the surface oxygen data used here are from 0 to 5 m while surface nutrients are taken between 0 and 10 m as those of 0–5 m present insufficient measurements (<2 monthly values per year) during 2014–16. A large number (2293) of surface oxygen observations are seen in the region during 2014–16, while that of nutrients data is much smaller (253) (Figure S1 in Supporting Information S1). Hence, we utilize an additional nutrients product with higher observational data coverage (3,402 samples in total and 743 ones for 2014–16) retrieved from ships of opportunity (SOO, https://www.bodc.ac.uk/data/published_data_library/catalogue/10.5285/7a7b497a-c47b-0a69-e053-6c86abc07ef0/). This is a unique data set with surface (5 m) nutrients concentrations collected monthly between May 2002 and October 2017 (Hartman et al., 2018). Full details on SOO sample collection and quality control can be found by Macovei et al. (2019). It can be noted that nutrients from the SOO data set cover most (∼64%) of the CA box and those from WOD18 are mainly in the northern part of the box (>51°N) (Figure S1 in Supporting Information S1).

The observation-based OceanSODA-ETHZ product (Gregor & Gruber, 2021) is considered for other biogeochemical data: pH, aragonite (Ω_{ar}) and calcite (Ω_{ca}) saturation states, dissolved inorganic carbon (DIC), and surface partial pressure of carbon dioxide ($spCO_2$). The OceanSODA-ETHZ data set is global and available from 1982 to 2022 on a monthly and 1 × 1° basis via https://www.ncei.noaa.gov/data/oceans/ncei/ocads/data/0220059/. This product uses measurements from ships and satellites and a machine learning clustering technique (Geospatial Random Cluster Ensemble Regression method) to accurately generate long-term and gap-free carbonate system parameters (Gregor & Gruber, 2021). This data set was previously used to quantify biogeochemical changes due to extreme ocean temperatures (Mogen et al., 2022). More details on OceanSODA-ETHZ are by Gregor and Gruber (2021).

2.2. Reanalysis Data

Daily fields of sea surface salinity (SSS) and mixed layer depth (MLD) are taken from the CMEMS Global Ocean Ensemble Reanalysis product over the period 1993–2020 (https://doi.org/10.48670/moi-00024). This global reanalysis has a ¼° resolution and 75 vertical levels (the depth range is from 0.5 to 5,902.1 m).

2.3. Calculation of Extremes Using Hobday MHW Framework

We detect MCS (MHW) in the North Atlantic (from 10 to 70°N) during 1982–2023 based on Hobday et al. (2016) definition as SST anomalous events cooler (warmer) than the 10th (90th) percentile for a duration exceeding 5 days and relative to a climatological period (1982–2011). FW and Salty Waves (SW, i.e., high salinity extremes) are calculated using the same statistical definition but during 1993–2020 and using 1995–2019 as the long-term mean period. This approach was recently applied to quantify global SSS extremes (Liu et al., 2023).

Following Oliver et al. (2018), for each extreme, we calculate six properties: The Frequency (annual number of extreme events), Total Days (annual total of extreme days), Duration (mean length (i.e., the time between the start and end dates of the event) and the Mean (MeanInt), Maximum (MaxInt) and Cumulative (CumInt) intensities (defined as average, maximum and integrated SST anomaly over the duration of the event, respectively). By combining the effects of duration and intensity, CumInt metric is useful in understanding the impacts on sensitive marine ecosystems as it is a measure of accumulated stress. For each of the extremes' metrics, we obtain annual means, a mean state (i.e., total mean) and annual linear trends for the period 1982–2023 (1993–2020) for MCS and MHW (FW and SW). Note that the method retrieves trends over the whole period extremes are calculated for and not per chunks of time.

2.4. Choice of Region

We identify the CA box (from 38 to 59°N and −42.5 to −16°E) (Figure 1) based on the MCS metrics spatial distribution in 2014–16 analyzed in Figure 4. This is because we investigate the CA region primarily as an expression of MCS and we focus specifically on the 2014–16 period. Noteworthy is that previous works (Josey et al., 2018; Sanders al., 2022) used different CA boxes, temperature data sets, and rationales behind the choice of region. The rationale behind the choice of region by Josey et al. (2018) is driven by the location of the maximum SST anomaly in 2015 and a focus on how it is affecting subsurface dynamics. The focus by Sanders et al. (2022) is on the cold anomaly within the mixed layer in 2015. In contrast, our motive is to calculate MCS, which requires daily SST data to encompass the full horizonal extent of the SST anomaly (as shown in Figure S2 in Supporting

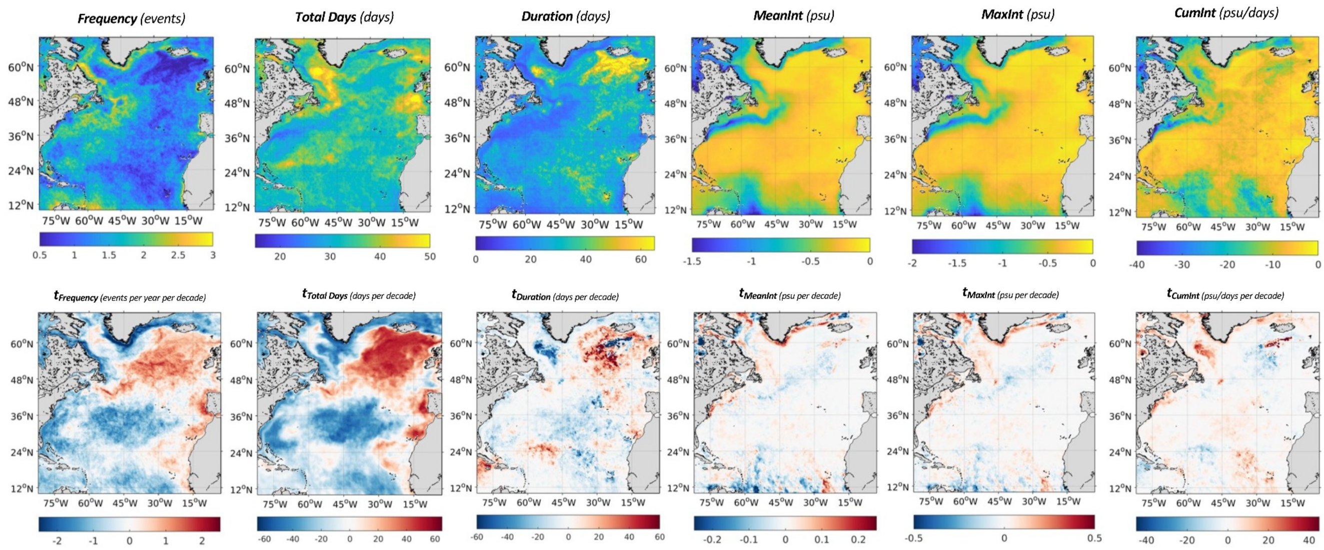

Figure 2. Same as Figure 1 but for FW and during 1993–2020.

Information S1). Hence, we use a different SST data product (with better-quality) than in the aforementioned papers. Indeed, Sanders et al. (2022) use SST from a model (ECCO) and compared to HadISST1.1 and Josey et al. (2018) use SST from HadISST1.1, whereas we use the OSTIA SST product. The OSTIA and HadISST1.1 SST products differ in their resolution, time period, and how they are produced. OSTIA has the advantage of higher spatial (0.05°) and temporal resolution (daily, which is needed to compute MCS) compared to HadISST1.1 (with a coarse 1° spatial resolution and a monthly frequency which does not allow to compute MCS).

Although, Josey et al. (2018) chose a CA box (extending latitudinally from 48 to 58°N, see their Figure 3a) that is about the upper half of our region, their SST cold anomaly spatial spread extends to the limits of our box. Sanders et al. (2022) CA box covering latitudes 43 to 63°N (see their Figure 1) was larger than that by Josey et al. (2018) but is of a similar size (with a slight northern shift) compared to our box. In both papers, only the 2015 SST anomaly map was used. Overall, our choice of CA region is consistent with previous definitions in the literature (Josey et al., 2018; Sanders et al., 2022) and the SST annual anomalies spatial distribution during 2014–16 (Figure S2 in Supporting Information S1). Furthermore, MCS calculated over the area used by Josey et al. (2018), which is the most different from our choice of region, led to similar results (not shown). However, it is unclear how a full

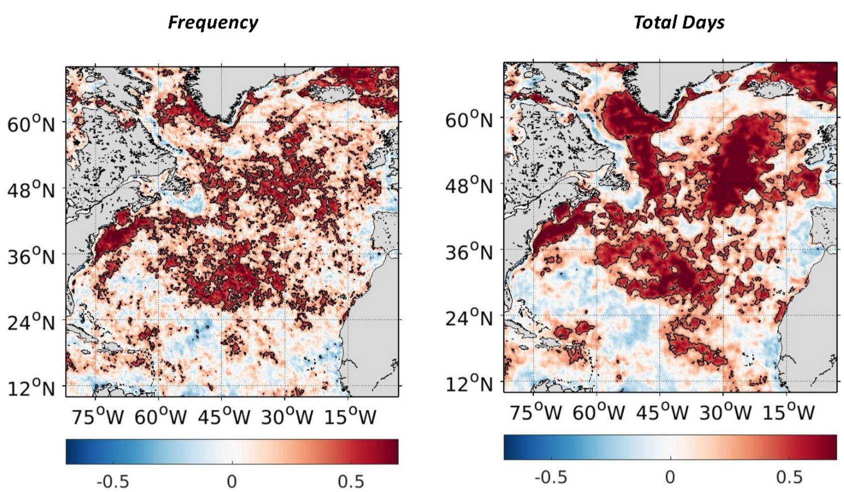

Figure 3. Spatial correlations between FW and MCS Frequency and Total Days during 1993–2020. Significant correlations at the 95% level are indicated by black contours.

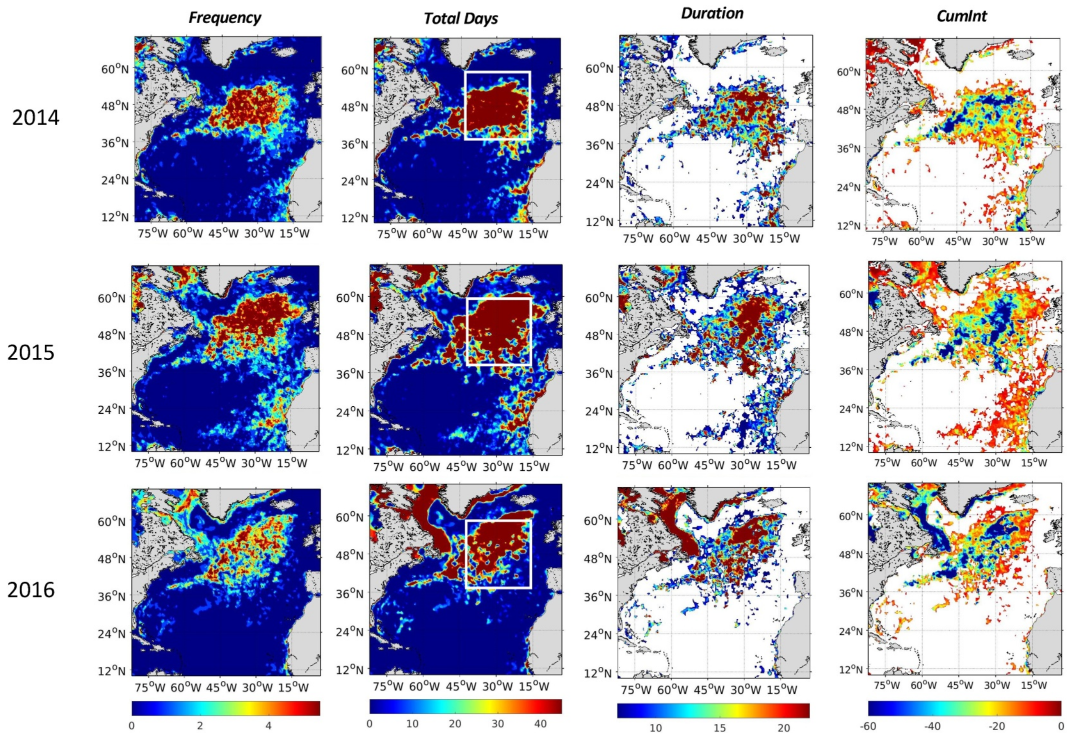

Figure 4. MCS Frequency, Total Days, Duration, and CumInt spatial distributions from 2014 to 2016. The white box indicates the horizontal extent of the CA region.

picture of the biogeochemical response can be obtained as few nutrients' data are available over the smaller region (used in Josey et al., 2018) as shown in Figure S1 in Supporting Information S1.

3. Results

3.1. MCS and FW Mean State, Trends, and Co-Occurrence

To examine and categorize properly the CA region in terms of MCS and FW, we analyze the findings in the context of the broader North Atlantic region (10–70°N). Hence, this section starts with a general analysis of the MCS and FW over the wider North Atlantic and where these extremes are prominent, followed by a focus on how the MCS and FW over the CA region compare to those areas, and ends with a highlight of how the CA region stands out in terms of MCS and FW.

A general overview of the MCS maps over the North Atlantic reveal that detected MCS manifest over a number of hotspot regions in the North Atlantic, such as the western Labrador Sea, South of Greenland, the Gulf stream path and also the CA region, our region of interest (Figure 1). Over the 42 years of observations (1982–2023), the most frequent (>3 events) MCS with the longest duration (>22 days) and total days (>45 days per year) in the North Atlantic (excluding Hudson Bay) are seen northeast of the Gulf Stream and in the subpolar and north subtropical regions, where the CA region stands out as the most pronounced for these metrics (Figure 1). The strongest MCS MeanInt (<−3.5°C), MaxInt (<−4°C), and CumInt (<−60°C/day) are observed in the Gulf Stream region, which is one of the global MCS hotspots (Jacobs et al., 2024; Schlegel et al., 2021) followed by the subpolar and north subtropical regions that include the Labrador Sea and CA region (Figure 1).

The 1982–2023 trends in MCS Frequency and Total days are overall significantly ($p_{\text{value}} < 0.05$) negative (about −1.5 event per decade and −20 days per decade, respectively) in the North Atlantic except in the western Labrador Sea, northeast of the Gulf Stream, and the CA region where they show a slight increase in Total days and no significant change in Frequency (Figure 1 and Figure S3 in Supporting Information S1, top row). MCS Duration trend is significantly ($p_{\text{value}} < 0.05$) increasing in the western Labrador Sea (>15 days per decade) along Greenland southeast coast (>10 days per decade) in 7% of the CA region (>8 days per decade) and south of 24°N

(3–5 days per decade) and is mainly negative over 24–36°N (−5 days per decade) except near the coasts and for West Africa upwelling zone (Figure 1 and Figure S3 in Supporting Information S1). MCS MeanInt and MaxInt show a significant increase (0.25 to >0.5°C per decade, $p_{\text{value}} < 0.05$) over the subpolar gyre, that is most pronounced south of Greenland, and a significant decline (<−0.5°C per decade, $p_{\text{value}} < 0.05$) over the Gulf Stream region (Figure 1 and Figure S3 in Supporting Information S1). The CumInt is also rapidly increasing (>15°C/day per decade, $p_{\text{value}} < 0.05$) over most of the subpolar gyre and the subtropics (south of 38°N) but shows a significant decline (<−15°C/day per decade, $p_{\text{value}} < 0.05$) in the western Labrador Sea, northeast of the Gulf Stream, and part of the CA region (Figure 1 and Figure S3 in Supporting Information S1). In summary, for the CA region, MCS trends during 1982–2023 reveal a slight increase in Duration (7% of the CA region), a (scattered) decline in the CumInt, minimal changes in the MeanInt and MaxInt, and no noticeable change in Frequency and Total days. Compared to the rest of the North Atlantic, the CA region does not exhibit any standout decadal trends in these metrics over this period.

North Atlantic (excluding Hudson Bay) FW for 1993–2020 appears the least (<0.5 events per year) in the Northeast Atlantic and much of the CA region, whereas they are most frequent (>3 events) in the Northwest Atlantic (Figure 2). FW Total Days (>50 days per year) are highest in the Labrador Sea, Northeast Atlantic and subtropics (24–35°N) and of medium magnitude (35 days per year, which is midrange compared to the scale used in the Total Days map and is about 58% the highest Total days) over the CA region. The Duration is longest (>65 days) over parts of the CA region and south of Iceland (Figure 2). FW exhibit high values in the MeanInt (<−1.5 psμ) and MaxInt (<−2 psμ) over the Gulf Stream region, the western Labrador Sea, along Greenland coasts and in the tropics (south of 24°N) (Figure 2). The CumInt displays a similar pattern but with a pronounced signal (−15 psμ/day) over the CA region and south of Iceland (Figure 2).

Interestingly, FW 1993–2020 trends show a significant ($p_{\text{value}} < 0.05$) increased Frequency (>2.5 events) and Total Days (>65 days per year) over the CA region and most Northeast Atlantic versus an overall significant ($p_{\text{value}} < 0.05$) decline in both metrics (<−2.5 days and <−65 days per year, respectively) over the rest of North Atlantic (Figure 2 and Figure S3 in Supporting Information S1). Trends in FW Duration are positive (>60 days) over most of the CA region and south of Iceland but are mainly negative (<−50 days) over the remaining areas (Figure 2). The MeanInt and MaxInt show a weak change (±0.1 psμ per decade) over most (~73%) of the North Atlantic and similarly for the CumInt except in the Labrador Sea where there is an increasing trend (40 psμ/day per decade) (Figure 2 and Figure S3 in Supporting Information S1). The MeanInt and MaxInt over the CA region display a weak negative trend (around −0.05 psμ per decade) that is significant ($p_{\text{value}} < 0.05$) for 11% the CA area. Generally, for the CA region, FW trends show increased frequency, Total days, and duration with overall lower intensity during 1993–2020.

The fact that MCS and FW have two different time periods constitutes a limitation. However, MCS metrics calculated over the same time span (1993–2020) as the FW reveal a similar pattern to those of 1982–2023 (with areas of strongest signal around the Gulf Stream path, subpolar and north subtropical regions and the CA region) but with overall reduced magnitude (Figure 1 and Figure S4 in Supporting Information S1). This is expected as both 1982–2023 and 1993–2020 MCS metrics are calculated relative to the same climatological period (1982–2011). However, the most prominent difference is seen in the MCS trends rather than the mean states (Figure 1 and Figure S3–S4 in Supporting Information S1). This is especially pronounced over the CA region with a strong and significant ($p_{\text{value}} < 0.05$) increasing trend in MCS Frequency (>2 events per decade), Duration (>15 days per decade), and Total days (>50 days per decade) and mainly a strong and significant ($p_{\text{value}} < 0.05$) decreasing trend in the CumInt (<−15°C/day per decade), MaxInt (<0.4°C) and MeanInt (<0.5°C). This difference in the trend indicates more frequent and long-lasting but less intense MCS over the CA region during 1990–2010s than in 1980s–early 2020s. This constitutes an interesting result for extremes calculation in general that changing the time period would affect primarily the trends of the extremes.

Overall, the CA region stands out with a tendency for more frequent, long-lasting, and less intense MCS and FW during 1993–2020 in comparison to other parts of the North Atlantic such as the Gulf Stream region, which exhibits more intense but less frequent and short-lasting MCS and FW during the same period (Figures 1 and 2). To further gain insight into the potential co-occurrence of these extreme events, a spatial point-by-point correlation between MCS and FW metrics during 1993–2020 is computed. Strong positive and significant (at the 95% level) correlations are seen in the Frequency and Total days metrics over the subpolar and subtropical regions with coefficients exceeding 0.7 in the Labrador Sea, mid Atlantic, north of the Gulf Stream and over the CA region

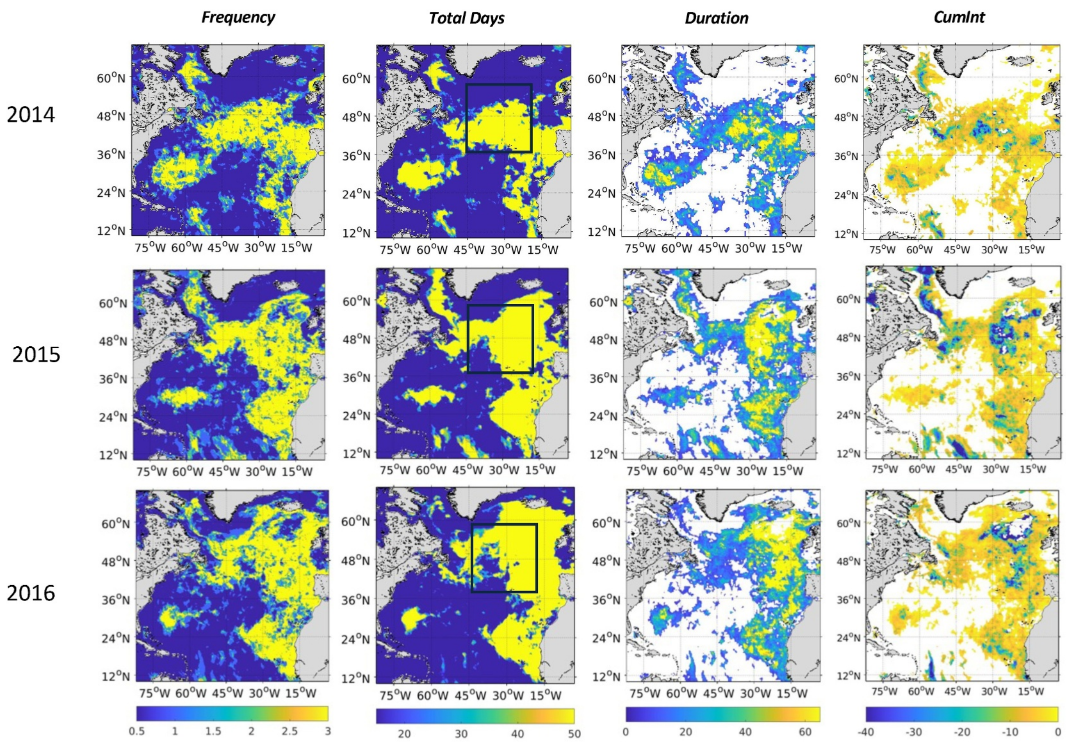

Figure 5. Same Figure 4 but for FW and the CA box are displayed in black.

(Figure 3). This supports the hypothesis that MCS and FW events can potentially be compound MCS-FW events in those parts of the North Atlantic.

3.2. MCS and FW Spatiotemporal Variability Over the CA Region During 2014–16

The strongest signal in the spatial distributions of annual MCS Frequency, Total Days, Duration, and CumInt from 2014 to 2016 is seen over the CA area with highly frequent (>5 events per year), long lasting (on average exceeding 45 days a year in total), and intense (<−60°C/days) events (Figure 4). Based on these MCS metrics delineations, we define the CA box as the area extending from 38 to 59°N and from −42.5 to −16°E (see Methods for more details on the choice of region). Overall, from 2014 to 16, MCS are well associated with FW indicating cool and fresh waters over the CA region (Figures 4 and 5). However, the FW pattern is more widespread than the MCS one, which is concentrated over the CA region to cover more areas of the Northeast Atlantic in addition to a large part of the CA region (Figure 5). This aligns with earlier suggestions that the unusual 2014–16 cooling contributed to a large redistribution of freshwater in the North Atlantic (Holiday et al., 2020). Over the CA region, FW metrics reveal low salinity events as frequent as >3 events per year, lasting for up to >140 days a year in total and up to >65 days per event, and as intense (in CumInt) as <−40 psμ/days (Figure 5) from 2014 to 16.

Timeseries of MCS and FW metrics over the selected CA location show that 2014-16 was one of the strongest events on record (Figure 6). In fact, the CA region's FW of 2014–16 had the longest number of Total Days (up to 148 days) and Duration (62 days), the strongest CumInt (down to −13 psμ/day) and (excluding 2012) was the most frequent (up to 2.8 events) for the whole period of 1993–2020 (Figure 6). FW of 2016 lasted the longest totaling about 148 days, which is 4.6 months (38.3% of the year), followed by 2015 with nearly 135 days (37% of the year) and then 2014 with ~70 days (19.2% of the year) (Figure 6). In terms of MCS timeseries in the CA region, they exhibit an overall stronger cooling (based on the Frequency, Total Days, and Duration metrics) in the 1980s (especially around 1985) than during 2014–16 event (Figure 6). However, the 2014-16 period shows the highest Frequencies (up to 4 events) and Total Days (up to 85 days) for 1995–2023 and the longest durations (up to 20 days) and strongest CumInt (down to −34°C/day) for 1993–2023 (Figure 6). MCS of 2015, the strongest in 2014–16 was the largest event in Duration, CumInt, and the second largest in Total Days during the 42 years of observations. The 2015 MCS continued for nearly 85 days that is about 3 months covering 23.3% of the year,

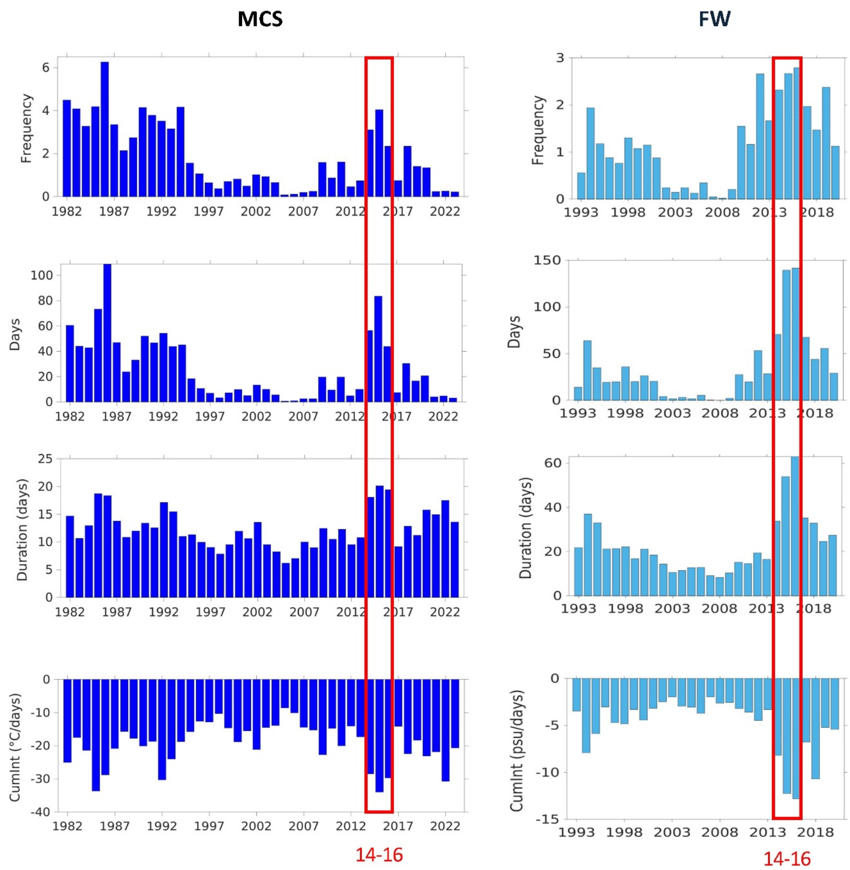

Figure 6. Timeseries of MCS and FW Frequency, Total Days, Duration, and CumInt from 1982 to 2023 and 1993 to 2020, respectively. Note that the vertical axes differ for MCS and FW metrics. Metrics of 2014–2016 are highlighted with a red rectangle.

while those of 2014 and 2016 lasted for a total 55 and 42 days (i.e., 15% and 11.5% of the year), respectively (Figure 6). Generally, for the period where both MCS and FW metrics are available (1993–2020), there is a coherent temporal variability (high significant correlations of the order of 0.6–0.74, $p_{\text{value}} < 0.05$) with 1990 and 2010s being cooler and fresher than the 2000s (Figure 6).

Noteworthy is that the MCS and FW annual metrics temporal variability during 1982–2023 and 1993–2020 over the CA region is complementary to that of the MHW and Salty Waves (SW, i.e., high salinity extremes) (Figure 6 and Figure S5 in Supporting Information S1). The periods of lows in MCS and FW metrics correspond generally to highs in MWH and SW metrics and vice versa. This suggest that the CA region has been oscillating between a cool and freshwater regime to a warm and salty water regime at least since 1993. Extrapolating back to 1982 for the MCS-MHW and based on the well-known Great Salinity Anomaly (extreme freshening events) of the 80s and early 90s (occurring around 1980–1983 and from around 1989 to 1995) in the subpolar the North Atlantic (e.g., Biló et al., 2022, their Figure 1c) which correspond here to occurrences of MCS (Figure 6), it is likely that this quasiperiodic pattern has been occurring since 1982. Furthermore, MHW and SW Frequency and Total Days show high positive significant (at the 95% level) spatial correlations (>0.7) over the CA region and the wider the North Atlantic (Figure S6 in Supporting Information S1). This is akin to the strong likelihood for co-occurrence between MCS and FW (Figure 3) further highlighting the pronounced complementary behavior between MCS-FW and MHW-SW in this region.

3.3. Vertical Mixing and Biogeochemical Response

Changes in temperature and salinity, such as the occurrence of MCS and FW, are likely to lead to changes in stratification and mixing conditions, impacting the biological productivity. As the CA box spans both subtropical

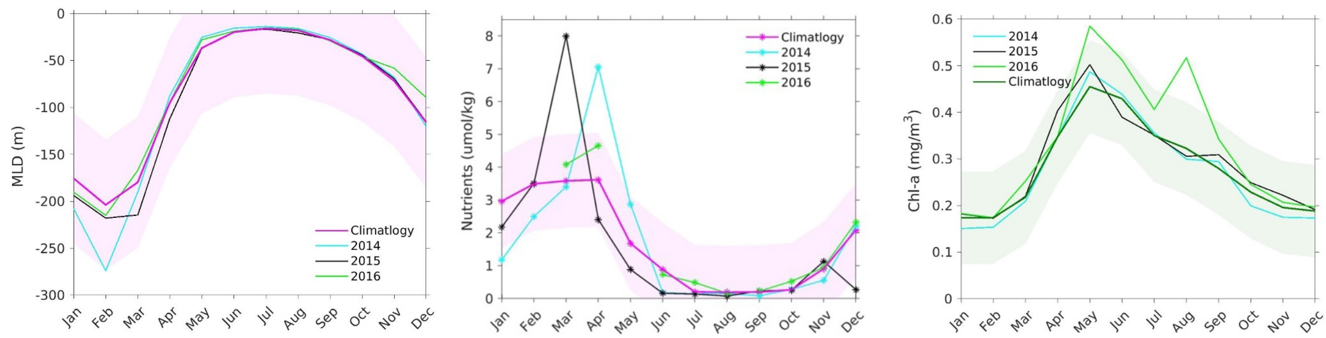

Figure 7. The seasonal cycles for MLD, nutrients (NO_2 and NO_3 from SOO data), and Chl-a averaged over the CA boxed region for the long-term mean and 2014 to 2016. The MLD long-term mean is from 1993 to 2020, the nutrients long-term mean is from 2002 to 2017, and the Chl-a long-term is from 1998 to 2022. Both the MLD and Chl-a are on from daily data sets that are averaged to monthly means to derive the long-term means. The light shading represents ±2 standard deviation from the long-term mean.

to subpolar regions, where vertical mixing is a key nutrient supply mechanism (e.g., Racault et al., 2017), we investigate the mechanistic link between changes in the MLD (as an indicator of vertical mixing), nutrients, and Chl-a (as a proxy for phytoplankton growth) relative to the long-tern mean conditions and in 2014–16.

The climatological seasonal cycles over the CA box show a MLD variability range that deepens down to 275 m in February with low minimum nutrients concentration (<0.5 μmol/kg in summer months, i.e. June, July, August) and Chl-a maximum values of up to 0.55 mg/m^3 in May (Figure 7 and Figure S7a in Supporting Information S1). Note that, for ease of analysis, we focus on the SOO data because it covers most (~64%) of the CA area and shows the same seasonal variability pattern as the WOD18/WOA23 nutrients data in the long term (i.e., increase in winter and decrease in summer months) and the years of interest (i.e., higher concentrations in 2014–16 than normal). The WOD data also show a similar seasonal cycle but details on specific seasonal differences in nutrient products are in Text S1 in Supporting Information S1. As MLD deepens, nutrients increase, leading to elevated Chl-a when the MLD subsequently shallows, with the strongest significant (P_{value} < 0.05) correlations being positive reaching values of 0.873 for MLD-nutrients at 1-month lag (i.e., nutrients lagged 1 month behind MLD), 0.774 for nutrients-Chl-a at 3-month lag, and 0.741 at 4-month lag for MLD-Chl-a (Figure 7 and Figure S7b in Supporting Information S1). In winter, enhanced mixing (deep MLD, Figure 7) brings nutrient-rich subsurface waters to the surface layers (Figure 7); however, it also causes phytoplankton to remain mixed over a greater depth and away from the sunlit surface. Combined with generally low shortwave radiation during winter, this results in low phytoplankton concentrations. During spring restratification in March–April, a shallow MLD keeps phytoplankton in the surface layers, where they are exposed to increased shortwave radiation and nutrients still enhanced after winter. This creates favorable conditions for the development of an enhanced phytoplankton bloom, which diminishes once the nutrients are exhausted in summer. All this is indicative of a system that is strongly limited by light during winters and nutrient-limited for phytoplankton growth in summer typical of the subtropics (e.g., Racault et al., 2017). However, other mechanisms driving the biophysical interactions could be at play given that the CA box (Figure 1) includes both subpolar and subtropical dynamics (see Discussion).

During the 2014-16 MCS over the CA region, we observe a deeper than normal MLD and higher nutrients and Chl-a than the long-terms means (Figure 7 and Figure S7a in Supporting Information S1), indicating more productive waters overall. The lead-lag relationship between MLD, nutrients, and Chl-a observed in the long-term mean exists also for 2014–16 (Figure 7 and Figure S7a in Supporting Information S1). Noteworthy is that overall, the maximum deepening of the MLD does not necessarily correspond to the maximum magnitude of the SST anomalous cooling over the CA region for 2014–16 and the long-term mean (Table S1 in Supporting Information S1). This is likely due to the processes driving the re-emergence of the cold anomaly from below the mixed layer as exemplified for 2015 by Sanders et al. (2022) in their Figure 8. The largest MLD change of 2014–16 is seen in 2014 with deepening down to 275 m (reached in February), which is quite significant as it sits at the lower edge of the ±2 standard deviations from the long-term mean envelope (Figure 7a). The deeper MLD in 2014 coincided with a high level of nutrients up to 7 μmol/kg (reached in April) that is twofold the normal level (Figures 7a and 7b). Chl-a concentrations in 2014 remain higher than normal one third of the year with the highest value (0.48 mg/m^3) recorded in May (Figure 7c). The second deepest MLD values are seen in 2015, descending to

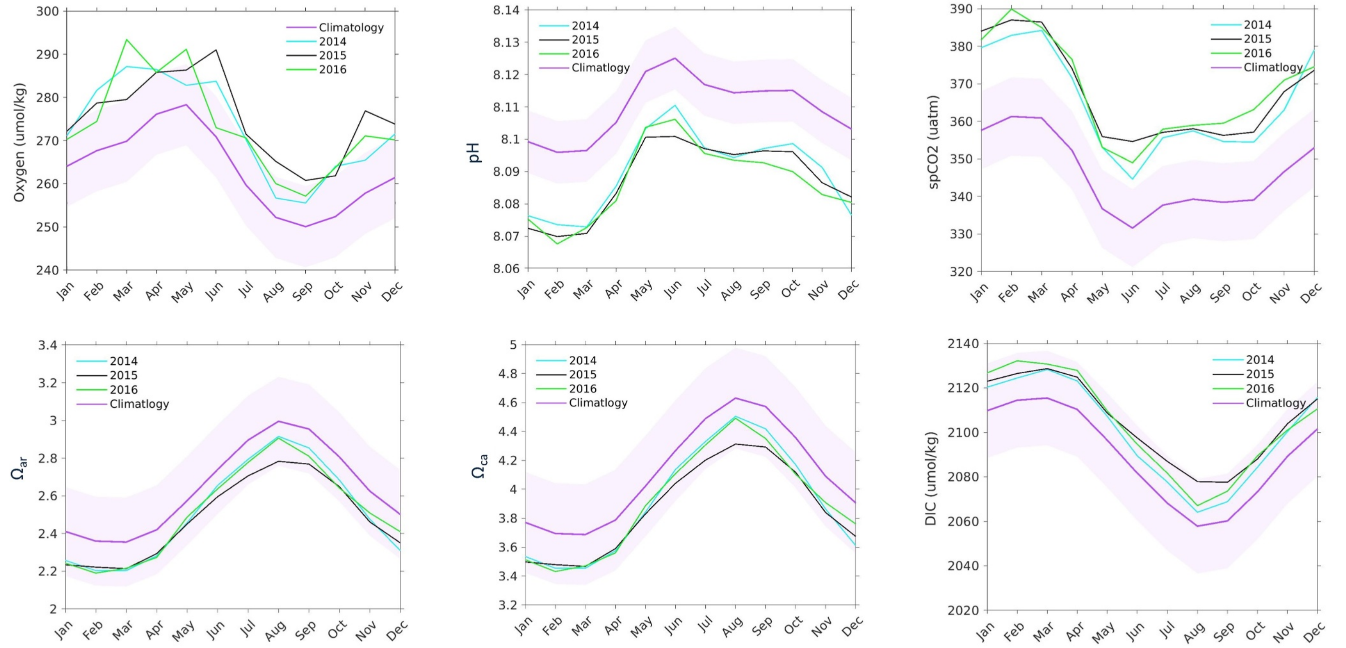

Figure 8. Same as Figure 7 but for oxygen, pH, $spCO_2$, DIC, Ω_{ac}, and Ω_{ar} and the long-term mean is from 1982 to 2022. These biogeochemical parameters are available months (see Methods for more details).

230 m in March (35% deeper than normal), associated with elevated nutrients reaching 8 μmol/kg in March which is 2.3 times the normal and the highest level in 2014–16 (Figure 7). Chl-a values in 2015 are greater than normal 75% of the time reaching a maximum of 0.5 mg/m^3 in May that constitutes a 10% increase (Figure 7c). The deepening of the MLD and increase in nutrients in 2016 were the smallest (10% deeper MLD in February and 28% higher nutrients in April) compared to those of 2014 and 2015 (Figure 7). However, Chl-a levels in 2016 exhibit the highest concertation of 2014–16, which prevail higher than normal all year round exceeding ±2 standard deviations in May and August (Figure 7c) (see Discussion for more details on mechanisms). In May 2016, Chl-a reached an absolute maximum of 0.58 mg/m^3 representing a 16% increase from the long-term mean (Figure 7c).

In addition to impacts on nutrients and phytoplankton productivity, we assess the impact on other biogeochemical parameters, namely oxygen, pH, Ω_{ar}, Ω_{ca}, DIC, and $spCO_2$. These parameters present marked seasonal cycles over the CA region in normal conditions (i.e., over the long-term mean) with oxygen increasing from 250 μmol/kg in September to 275 μmol/kg in May followed by a decrease during the rest of the year, and pH levels oscillating from 8.097 in February up to 8.125 in June after which it has an overall decrease (Figure 8). The long-term mean in $spCO_2$ over the CA region peaks from around 330 μatm in June to around 360 μatm in February–March dropping down between March–April and May–June (Figure 8). Both Ω_{ar} and Ω_{ca} long-term means show an increase from March to August followed by a reduction during the remaining months (Figure 8). DIC long-term mean levels over the CA region range from a maximum of 2170 μmol/kg in March to a minimum of 2055 μmol/kg in August (Figure 8). The CA region in 2014–16 is characterized by anomalously high oxygen with values up to 295 μmol/kg (11% increase) and exceeds 2 standard deviations most of the year (7–9 out of 12 months) compared to the long-term mean (Figure 8). This suggests that MCS likely increased oxygen levels, which is expected since cooler water enhances oxygen uptake. Less alkaline conditions are observed during 2014–16 with a significant (exceeding 2 standard deviations from the climatological mean) decrease in pH down to 8.07 (Figure 8). Likewise, Ω_{ar} and Ω_{ca} show an overall reduction albeit not below the −2 standard deviations from normal, indicating an exacerbation of ocean acidification during 2014–16 (Figure 8). These more acidic conditions could be in part due to the influence of FW (low salinity), since freshwater can make the ocean more vulnerable to acidification (e.g., Thomas et al., 2021). Similarly, the re-emergence of the cold anomaly from beneath the mixed layer, as described above, would bring lower pH waters to the surface further enhancing acidification during MCS. The CA region is also characterized by anomalously high $spCO_2$ in 2014–16 by more than 2 standard deviations from the long-term mean reaching a maximum of 390 μatm (Figure 8), which is unsurprising as colder waters take up more CO_2 than warmer waters. The region DIC surface level shows an overall increase for 2014–16 up to maxima of 2120–2130 μmol/kg that is at the upper edge of the ±2 standard deviations envelope (Figure 8). This can be anticipated as cooler water increases DIC levels since it enhances the solubility of carbon dioxide.

4. Discussion and Conclusions

In this study, we characterize the North Atlantic CA region (also known as the cold blob region) signal from an MCS and FW perspective and quantify the biogeochemical response at the surface during 2014–16. Our findings reveal a quasi-periodic nature to the MCS and FW over the CA region (from the 80s to early 20s) characterized by shifts from cool and freshwater conditions to a warm and salty water regime. Interestingly, similar cycles of variability were reported at the Porcupine Abyssal Plain Sustained Observatory (PAP-SO) site (Figure S8 in Supporting Information S1, Lampitt et al., 2023), albeit it is a single observational point, and the salinity changes agree with recent model-based results in the wider eastern subpolar gyre (Siddiqui et al., 2024). Since the 1990s, MCS and FW seem to be co-occurring over this region with a higher frequency, longer periods but weaker compared with other parts of the North Atlantic. Note that, here, only the potential co-occurrence of MCS and FW events is explored and a future "compound extreme events" analysis (e.g., Le Grix et al., 2021) is needed to confirm entirely that they occur simultaneously. It is also worth noting that this study does not address the seasonality of MCS and FW as the applied Hobday et al. (2016) approach retrieves only annual metrics and not seasonal ones (i.e., a metric per year but not per season for each year). The seasonality of MCS and FW over the region remains to be examined in a future study, as it requires a different approach (e.g., Jacox et al., 2022; Wang & Zhou, 2024) and there seems not to be a consensus on a common methodology for this. We showed that the Atlantic CA region in 2014–16 experienced one of the most widespread and long-lasting (for 3–4.6 months) MCS and FW ever recorded, co-occurring with a deeper mixed layer and resulting in a distinct biogeochemical signature (compared to the long-term mean). It shows increased oxygen levels (which is expected since cooler waters enhance oxygen uptake), elevated $spCO_2$, lower aragonite and calcite saturation states, and a significant decrease in pH, indicating intensified ocean acidification (that could be in part due to the influence of FW as freshwater leads to lower resistance to acidification). Another noticeable element in this response is the nutrient-rich and well-oxygenated waters as well as the overall elevated phytoplankton biomass compared to normal. This more productive system during 2014–16 MCS over the CA region contributes to a further increase in oxygen levels. However, at the same time, photosynthesis by phytoplankton removes CO_2 from seawater, reducing carbonic acid concentration and increasing pH. Consequently, Ω_{ar} and Ω_{ca} would also rise, as lower CO_2 levels reduce bicarbonate and hydrogen ion concentrations increasing carbonate ion availability. This increase in Ωar and Ωca and pH counteracts the decline caused by freshening. However, the overall trend found here remains a decline in these variables (Ω_{ar} and Ω_{ca} and pH), suggesting that the freshening mechanism (due to FW) is dominant. Similarly, the impact of increased productivity could lead to a decrease in DIC and $spCO_2$ levels, counteracting the effect of cool temperatures. However, the observed overall increase in $spCO_2$ suggests that cool temperatures (MCS) is the dominant mechanism. Additionally, the enhanced respiration (elevated O2) is another factor leading to the observed increase in DIC (which also contributes to ocean acidification) and $spCO_2$ levels. Noteworthy is the increased Chl-a presents a varying interannual signal between 2014 and 16. Indeed, the fact that the largest phytoplankton biomass in 2014–16 was when the MLD deepening was the smallest and the nutrients concentrations (based on SOO data) the lowest (2016 timeseries in Figure 7) suggest as expected that this interannual variability is of a system that is strongly limited by light as well as nutrients. The 2014-16 MCS over the CA region are associated with a deepening of the MLD during the winter months in turn causing a lagged increase in nutrients and Chl-a in spring months. As shown in previous work, MLD reached a maximum deepening in winter 2015 associated with a freshening (Holiday et al., 2020; Sanders et al., 2022). The freshening suggests that interannual deepening of the winter MLD was driven by stronger temperature-driven convection with salinity changes promoting stratification of the mixed layer (Sanders et al., 2022). MCS co-occurrence with high nutrients and phytoplankton biomass can be explained by the fact that MCS may represent a surface expression of cool waters trapped below the mixed layer. Indeed, the process of re-emergence (by which SST anomalies are stored beneath the mixed layer then brought back up to the surface as the mixed layer deepens) was shown to be key in sustaining the anomalous cooling over the CA region (Sanders et al., 2022). Weaker summer surface warming of the mixed layer led to maximum temperature cooling over the CA region in 2015 (See Figures 8; Sanders et al., 2022, for details). There might be other factors responsible for the productivity in addition to nutrients supply from vertical mixing. Factors such as changes in light conditions (typical of subpolar regions) and/or changes in zonal currents (particularly in the subtropics), which can lead to enhanced horizontal advection of nutrients, and in turn, phytoplankton growth (e.g., Carracedo et al., 2021; Racault et al., 2017). As mentioned previously, the CA box stretches across parts of the subpolar and subtropical gyres, so there could be distinct MLD, nutrients, and Chl-a responses within the box itself. This is indirectly suggested by the dissimilarity in magnitude between the SOO and WOA23 nutrients climatologies and in 2014–16 as they cover different parts of the CA box (Figure 7, Figure S7a and Text S1 in Supporting Information S1). To fully examine these mechanistic links, an in-depth analysis with a model experiment (out of the scope of this study) is required and will be investigated in future research. Likewise, a model-based study would help understand subsurface changes in both physical and biogeochemical parameters. Other caveats to our analysis are that the nutrients data are limited and we are using remotely sensed Chl-a, which serves only as a proxy for total phytoplankton biomass. It does not account for the significance of phytoplankton size structure or the differences in growth rates and nutrient requirements between larger and smaller phytoplankton types (e.g., Maranon, 2015). Therefore, further research involving more detailed in situ measurements and/or biogeochemical models is needed to provide a more nuanced understanding of the biogeochemical responses to the MCS over the CA region.

Comparing the physical dynamics and biogeochemical response of the Atlantic's CA region in 2014–16 to those of the Pacific's warm anomaly (also known as the Pacific blob or warm blob) which occurred at the same time (2014–16), we notice striking mirroring effects. Indeed, in 2014–16, the cold blob manifests as an MCS and FW (Figures 1–4), whereas the Pacific blob is detected as an MHW (e.g., Bond et al., 2015) with positive salinity anomalies (i.e., saltier waters than normal) (Holser et al., 2022; Scannell et al., 2020). The MLD is deeper than normal for the CA region indicating well-mixed water (Figure 7). In contrast, it was reported that the Pacific warm anomaly led to increased stratification (Mogen et al., 2022). Although more oxygenated waters are observed over the CA region (Figure 8), low oxygen conditions prevailed in Pacific blob (Mogen et al., 2022). The higher DIC and lower Ω_{ar} of the CA region coincided with a decrease in DIC and reprieve of ocean acidification in the warm blob (Mogen et al., 2022). Though these opposite effects between 2014 and 16 Atlantic cold and Pacific warm anomalies could be a mere coincidence, as they are occurring in two different ocean basins previous research proposed the existence of a common atmospheric driver between the two phenomena (Josey et al., 2018; Liang et al., 2017). Specifically, Liang et al. (2017) showed that the Tropical Northern Hemisphere (TNH) atmospheric pattern is a dominant mode of covariability in the North Pacific-Atlantic sector, linking the cold and warm anomalies in the long term (1950–2010s). The TNH pattern cross-basin structure acts as a forcing for SST variations in the Atlantic CA and Pacific warm blob regions, leading to instances where both anomalies occur simultaneously including for the 2014–16 event (Liang et al., 2017, their Figures 2 and 9). However, the contribution of the TNH pattern to the formation of the Pacific blob was found to be greater than that to the Atlantic CA region (Liang et al., 2017). The interconnection of the various climate modes (THN, NAO, AMO, EAP…) could also be at play and future research is needed to unravel fully their impact on the CA region.

Ecological impacts of the 2014–16 MCS over the CA region on marine species are still unclear probably due to its open ocean location where the necessary observations are less common (Schlegel et al., 2021). Despite a reduction of ocean acidification, the Pacific warm anomaly led to an intensified deoxygenation, productivity decline, and damaging impacts on the ecology such as widespread seals deaths and whale strandings and significant changes in seabird reproduction and fish distribution (Cavole et al., 2016; Cheung & Frölicher, 2020; Mogen et al., 2022; Suryan et al., 2021). Given the latter, the common conducting atmospheric pattern (Liang et al., 2017) and the strong antisymmetry of ocean physical effects and the biogeochemical response between Pacific and Atlantic anomalies (Figures 1–8; Mogen et al., 2022; Holser et al., 2022), it is possible to speculate that 2014–16 MCS over the CA region impacts might have been less severe or even beneficial for marine organisms. Generally, such effects on fish and higher trophic levels (e.g., increased abundance) are less likely to be reported or lead to complaints. This might be another reason for the absence of reports on the marine life impacts of the 2014–16 MCS over the CA region and remain to be investigated in a future work using fishing catch data like those provided by Sea Around Us and Global Fishing Watch web databases. However, MCS in general can severely disturb marine species distribution, migration patterns, abundance, phenology, and in extreme cases lead to mass mortality or sublethal effects such as suppressed growth (e.g., Schlegel et al., 2021 and references therein). For instance, an exceptional cooling in 1962–63 in the Northeast Atlantic massively impacted Sole species abundance causing a halving in the spawning-stock biomass (Millner & Whiting, 1996). Additionally, compound MCS and FW events over the CA region could amplify the ecological response as salinity extremes may cause high mortality rates among stenohaline species (Liu et al., 2023; Zhang et al., 2019). The 2014–16

MCS over the CA region has also exacerbated ocean acidification (Figure 8), which could be detrimental to marine species. The level of severity of MCS and FW ecological impacts depends on various factors including organisms' ability to tolerate these extremes (Grant et al., 2017; Liu et al., 2023). For cold-adapted species, MCS could serve as a buffer delaying the impact of rising temperatures and climate change (Feng et al., 2020; Schlegel et al., 2021). The quasiperiodic behavior of Atlantic's CA region and positive changes in some ecosystem indicators in 2014–16 (e.g., the rise in productivity, nutrients, and oxygen levels) highlight the need for ecological research assessing species displacement, recovery, and potential restoration through species relocation from warm to colder zones. This is especially relevant as the CA region encompasses five main Marine Protected Areas, hosting diverse species (including tuna, sharks, whales, and seabirds) and the PAP-SO site (Figure S8 in Supporting Information S1) with long-term timeseries. Such efforts could feed into the strategies of preparedness for future marine extremes in the North Atlantic.

Data Availability Statement

Publicly available satellite, reanalysis, and in situ data sets were used in this study. The satellite SST and Chl-a and reanalysis SSS and MLD are available from the CMEMS data portal (http://marine.copernicus.eu/services-portfolio/access-to-products/) under https://doi.org/10.48670/moi-00168, https://doi.org/10.48670/moi-00283 and https://doi.org/10.48670/moi-00024, respectively. The in situ SOO nutrient data are publicly available from the British Oceanographic Data Centre (Hartman et al., 2018). The in situ oxygen and nutrients profiles in WOD18 and WOA23 databases are available online (Boyer et al., 2016; Reagan et al., 2023). The OceanSODA-ETHZ data set is freely accessible (Gregor & Gruber, 2020).

Acknowledgments
The study was supported by the following UK National Capability projects: FOCUS (https://noc.ac.uk/projects/focus) under grant NE/X006271/1 and AtlantiS (https://projects.noc.ac.uk/atlantis/) under grant NE/Y005589/1. The satellite SST and Chl-a and reanalysis data were distributed by the CMEMS (http://www.marine.copernicus.eu). The SOO nutrient data are publicly available from the British Oceanographic Data Centre (https://www.bodc.ac.uk/data/published_data_library/catalogue/10.5285/7a7b497a-c47b-0a69-e053-6c86abc07ef0/). We thank ETH Zurich for developing OceanSODA-ETHZ data set and NOAA's National Centers for Environmental Information (NCEI) for collecting and providing the oxygen and nutrients profiles in WOD18 and WOA23 databases.

References

Biló, T. C., Straneo, F., Holte, J., & Le Bras, I. A.-A. (2022). Arrival of new great salinity anomaly weakens convection in the irminger sea. *Geophysical Research Letters*, *49*(11), e2022GL098857. https://doi.org/10.1029/2022GL098857

Bond, N. A., Cronin, M. F., Freeland, H., & Mantua, N. (2015). Causes and impacts of the 2014 warm anomaly in the NE Pacific: 2014 warm anomaly in the NE Pacific. *Geophysical Research Letters*, *42*(9), 3414–3420. https://doi.org/10.1002/2015GL063306

Boyer, T. P., Antonov, J. I., Baranova, O. K., Coleman, C., García, H. E., Grodsky, A., et al. (2016). NCEI standard product: World Ocean Database (WOD18). (nutrients and oxygen) [Dataset]. *NOAA National Centers for Environmental Information*. https://www.ncei.noaa.gov/archive/accession/NCEI-WOD

Boyer, T. P., Baranova, O. K., Coleman, C., Garcia, H. E., Grodsky, A., Locarnini, R. A., et al. (2018). In A. V. Mishonov (Ed.), *World Ocean database 2018*. NOAA Atlas NESDIS 87. Retrieved from https://www.ncei.noaa.gov/sites/default/files/2020-04/wod_intro_0.pdf

Brauko, K. M., Cabral, A., Costa, N. V., Hayden, J., Dias, C. E. P., Leite, E. S., et al. (2020). Marine heatwaves, sewage and eutrophication combine to trigger deoxygenation and biodiversity loss: A SW Atlantic case study. *Frontiers in Marine Science*, *7*, 590258. https://doi.org/10.3389/fmars.2020.590258

Bryden, H. L., King, B. A., McCarthy, G. D., & McDonagh, E. L. (2014). Impact of a 30% reduction in Atlantic meridional overturning during 2009–2010. *Ocean Science*, *10*(4), 683–691. https://doi.org/10.5194/os-10-683-2014

Carracedo, L. I., Mercier, H., McDonagh, E., Rosón, G., Sanders, R., Moore, C. M., et al. (2021). Counteracting contributions of the upper and lower meridional overturning limbs to the North Atlantic nutrient budgets: Enhanced imbalance in 2010. *Global Biogeochemical Cycles*, *35*(6), e2020GB006898. https://doi.org/10.1029/2020GB006898

Cavole, L. M., Demko, A. M., Diner, R. E., Giddings, A., Koester, I., Pagniello, C. M., et al. (2016). Biological impacts of the 2013–2015 warm-water anomaly in the Northeast Pacific: Winners, losers, and the future. *Oceanography*, *29*(2), 273–285. https://doi.org/10.5670/oceanog.2016.32

Cetina-Heredia, P., & Allende-Arandía, M. E. (2023). Caribbean marine heatwaves, marine cold spells, and co-occurrence of bleaching events. *Journal of Geophysical Research: Oceans*, *128*(10), e2023JC020147. https://doi.org/10.1029/2023JC020147

Cheung, W. W., & Frölicher, T. L. (2020). Marine heatwaves exacerbate climate change impacts for fisheries in the Northeast Pacific. *Scientific Reports*, *10*(1), 6678. https://doi.org/10.1038/s41598-020-63650-z

Colella, M. A., Ruzicka, R. R., Kidney, J. A., Morrison, J. M., & Brinkhuis, V. B. (2012). Cold-water event of January 2010 results in catastrophic benthic mortality on patch reefs in the Florida keys. *Coral Reefs*, *31*(2), 621–632. https://doi.org/10.1007/s00338-012-0880-5

Dalsin, M., Walter, R. K., & Mazzini, P. L. F. (2023). Effects of basin-scale climate modes and upwelling on nearshore marine heatwaves and cold spells in the California Current. *Scientific Reports*, *13*(1), 12389. https://doi.org/10.1038/s41598-023-39193-4

Di Lorenzo, E., & Mantua, N. (2016). Multi-year persistence of the 2014/15 North Pacific marine heatwave. *Nature Climate Change*, *6*(11), 1042–1047. https://doi.org/10.1038/nclimate3082

Duchez, A., Frajka-Williams, E., Josey, S., Evans, D., Grist, J., Marsh, R., et al. (2016). Drivers of exceptionally cold North Atlantic Ocean temperatures and their link to the 2015 European heat wave. *Environmental Research Letters*, *11*(7), 074004. https://doi.org/10.1088/1748-9326/11/7/074004

Feng, M., Caputi, N., Chandrapavan, A., Chen, M., Hart, A., & Kangas, M. (2020). Multi-year marine cold-spells off the west coast of Australia and effects on fisheries. *Journal of Marine Systems*, 103473.

Garcia, H. E., Bouchard, C., Cross, S. L., Paver, C. R., Wang, Z., Reagan, J. R., et al. (2024b). In A. Mishonov (Ed.), *World Ocean Atlas 2023, volume 4: Dissolved inorganic nutrients (Phosphate, Nitrate, Silicate)*. NOAA Atlas NESDIS 92.

Garcia, H. E., Wang, Z., Bouchard, C., Cross, S. L., Paver, C. R., Reagan, J. R., et al. (2024). In A. Mishonov (Ed.), *World Ocean Atlas 2023, volume 3: Dissolved oxygen, apparent oxygen utilization, and oxygen saturation* (Vol. 91). NOAA Atlas NESDIS.

Grant, P. R., Grant, B. R., Huey, R. B., Johnson, M. T. J., Knoll, A. H., & Schmitt, J. (2017). Evolution caused by extreme events. *Philosophical transactions of the royal society B: Biological sciences* (Vol. 372(1723), 20160146). https://doi.org/10.1098/rstb.2016.0146

Gregor, L., & Gruber, N. (2020). OceanSODA-ETHZ: A global gridded dataset of the surface ocean carbonate system for seasonal to decadal studies of ocean acidification (v2023) (NCEI accession 0220059) [Dataset]. *NOAA National Centers for Environmental Information*. https://doi.org/10.25921/m5wx-ja34

Gregor, L., & Gruber, N. (2021). OceanSODA-ETHZ: A global gridded data set of the surface ocean carbonate system for seasonal to decadal studies of ocean acidification. *Earth System Science Data*, *13*(2), 777–808. https://doi.org/10.5194/essd-13-777-2021

Hartman, S. E., Schuster, U., Macovei, V. A., & Hydes, D. J. (2018). Nitrate, silicate, and phosphate data from ships of opportunity in the North Atlantic 2002-2007 [Dataset]. *British Oceanographic Data Centre - Natural Environment Research Council*. https://doi.org/10.5285/7a7b497a-c47b-0a69-e053-6c86abc07ef0

Henson, B. (2016). The North Atlantic blob: A marine cold wave that won't go away. *WunderBlog, Weather Underground*. https://www.wunderground.com/blog/JeffMasters/the-north-atlantic-blob-a-marine-cold-wave-that-wont-go-away.html

Hobday, A. J., Alexander, L. V., Perkins, S. E., Smale, D. A., Straub, S. C., Oliver, E. C., et al. (2016). A hierarchical approach to defining marine heatwaves. *Progress in Oceanography*, *141*, 227–238. https://doi.org/10.1016/j.pocean.2015.12.014

Holbrook, N. J., Scannell, H. A., Sen Gupta, A., Benthuysen, J. A., Feng, M., Oliver, E. C. J., et al. (2019). A global assessment of marine heatwaves and their drivers. *Nature Communications*, *10*(1), 2624. https://doi.org/10.1038/s41467-019-10206-z

Holliday, N. P., Bersch, M., Berx, B., Chafik, L., Cunningham, S., Florindo-López, C., et al. (2020). Ocean circulation causes the largest freshening event for 120 years in eastern subpolar North Atlantic. *Nature Communications*, *11*(1), 585. https://doi.org/10.1038/s41467-020-14474-y

Holser, R. R., Keates, T. R., Costa, D. P., & Edwards, C. A. (2022). Extent and magnitude of subsurface anomalies during the Northeast Pacific Blob as measured by animal-borne sensors. *Journal of Geophysical Research: Oceans*, *127*(7), e2021JC018356. https://doi.org/10.1029/2021JC018356

IOCCG. (2000). Remote sensing of ocean colour in coastal and other optically complex waters. In *Reports of the international ocean colour coordinating group number 3* (p. 140). Sathyendrannath (Dartmouth, Canada). Retrieved from https://www.ioccg.org/reports/report3.pdf

Jacobs, Z. L., Jebri, F., Wakelin, S., Strong, J., Popova, E., Srokosz, M., & Loveridge, A. (2024). Marine heatwaves and cold spells in the Northeast Atlantic: What should the UK be prepared for? *Frontiers in Marine Science*, *11*. https://doi.org/10.3389/fmars.2024.1434365

Jacox, M. G., Alexander, M. A., Amaya, D., Becker, E., Bograd, S. J., Brodie, S., et al. (2022). Global seasonal forecasts of marine heatwaves. *Nature*, *604*(7906), 486–490. https://doi.org/10.1038/s41586-022-04573-9

Jentsch, A., Kreyling, J., & Beierkuhnlein, C. (2007). A new generation of climate-change experiments: Events, not trends. *Frontiers in Ecology and the Environment*, *5*(6), 315–324. https://doi.org/10.1890/1540-9295(2007)5[365:angoce]2.0.co;2

Josey, S. A., Hirschi, J. J.-M., Sinha, B., Duchez, A., Grist, J. P., & Marsh, R. (2018). The recent Atlantic cold anomaly: Causes, consequences, and related phenomena. *Annual Review of Marine Science*, *10*(1), 475–501. https://doi.org/10.1146/annurev-marine-121916-063102

Lampitt, R. S., Briggs, N., Cael, B. B., Espinola, B., Hélaouët, P., Henson, S. A., et al. (2023). Deep ocean particle flux in the Northeast Atlantic over the past 30 years: Carbon sequestration is controlled by ecosystem structure in the upper ocean. *Frontiers in Earth Science*, *11*. https://doi.org/10.3389/feart.2023.1176196

Le Grix, N., Zscheischler, J., Rodgers, K. B., Yamaguchi, R., & Frölicher, T. L. (2021). Hotspots and drivers of compound marine heatwaves and low net primary production extremes. *Biogeosciences*, *19*(24), 5807–5835. https://doi.org/10.5194/bg-19-5807-2022

Li, C., Huang, J., Liu, X., Ding, L., He, Y., & Xie, Y. (2024). The ocean losing its breath under the heatwaves. *Nature Communications*, *15*(1), 6840. https://doi.org/10.1038/s41467-024-51323-8

Liang, Y., Yu, J., Saltzman, E. S., & Wang, F. (2017). Linking the tropical northern Hemisphere pattern to the Pacific warm blob and Atlantic cold blob. *Journal of Climate*, *30*(22), 9041–9057. https://doi.org/10.1175/JCLI-D-17-0149.1

Liu, H., Xu, T., Li, D., Nie, X., & Wei, Z. (2023). Sea surface salinity extremes over the global ocean. *Environmental Research Letters*, *18*(11), 114020. https://doi.org/10.1088/1748-9326/ad0165

Lubitz, N., Daly, R., Smoothey, A. F., Vianello, P., Roberts, M. J., Schoeman, D. S., et al. (2024). Climate change-driven cooling can kill marine megafauna at their distributional limits. *Nature Climate Change*, *14*(5), 526–535. https://doi.org/10.1038/s41558-024-01966-8

Macovei, V. A., Torres-Valdés, S., Hartman, S. E., Schuster, U., Moore, C. M., Brown, P. J., et al. (2019). Temporal variability in the nutrient biogeochemistry of the surface North Atlantic: 15 years of ship of opportunity data. *Global Biogeochemical Cycles*, *33*(12), 1674–1692. https://doi.org/10.1029/2018GB006132

Maranon, E. (2015). Cell size as a key Determinant of phytoplankton Metabolism and community structure. *Annual Review of Marine Science*, *7*(1), 241–264. https://doi.org/10.1146/annurev-marine-010814-015955

Mattiasen, E. G., Kashef, N. S., Stafford, D. M., Logan, C. A., Sogard, S. M., Bjorkstedt, E. P., & Hamilton, S. L. (2020). Effects of hypoxia on the behavior and physiology of kelp forest fishes. *Global Change Biology*, *26*(6), 3498–3511. https://doi.org/10.1111/gcb.15076

Millner, R. S., & Whiting, C. L. (1996). Long-term changes in growth and population abundance of sole in the North Sea from 1940 to the present. *ICES Journal of Marine Science*, *53*(6), 1185–1195.

Mogen, S. C., Lovenduski, N. S., Dallmann, A. R., Gregor, L., Sutton, A. J., Bograd, S. J., et al. (2022). Ocean biogeochemical signatures of the North Pacific blob. *Geophysical Research Letters*, *49*(9), e2021GL096938. https://doi.org/10.1029/2021GL096938

Mohamed, B., Barth, A., & Alvera-Azcárate, A. (2023). Extreme marine heatwaves and cold-spells events in the Southern North Sea: Classifications, patterns, and trends. *Frontiers in Marine Science*, *10*. https://doi.org/10.3389/fmars.2023.1258117

Mooney. (2015). Mooney. Retrieved from https://www.washingtonpost.com/news/energy-environment/wp/2015/09/24/why-some-scientists-are-worried-about-a-cold-blob-in-the-north-atlantic-ocean/

Oliver, E. C. J., Donat, M. G., Burrows, M. T., Moore, P. J., Smale, D. A., Alexander, L. V., et al. (2018). Longer and more frequent marine heatwaves over the past century. *Nature Communications*, *9*(1), 1324. https://doi.org/10.1038/s41467-018-03732-9

Peal, R., Worsfold, M., & Good, S. (2023). Comparing global trends in marine cold spells and marine heatwaves using reprocessed satellite data. In K. vonSchuckmann, L. Moreira, P.-Y. Le Traon, M. Grégoire, M. Marcos, J. Staneva, et al. (Eds.), *7th edition of the Copernicus Ocean State Report (OSR7)*. Copernicus Publications, State Planet. https://doi.org/10.5194/sp-1-osr7-3-2023.1osr73.

Racault, M. F., Sathyendranath, S., Brewin, R. J. W., Raitsos, D. E., Jackson, T., & Platt, T. (2017). Impact of El Nino variability on oceanic phytoplankton. *Frontiers in Marine Science*, *4*, 133. https://doi.org/10.3389/fmars.2017.00133

Rahmstorf, S., Jason, E. B., Feulner, G., Mann, M. E., Robinson, A., Rutherford, S., & Schaffernicht, E. J. (2015). Exceptional twentieth-century slowdown in Atlantic Ocean overturning circulation. *Nature Climate Change*, *5*, 475–480. https://doi.org/10.1038/nclimate2554

Ramirez Grand. (2023). Ramirez Grand. Retrieved from https://loopbottles.com/en-int/blogs/notizie/il-blob-freddo-dellatlantico-un-mistero-oceanografico

Reagan, J. R., Boyer, T. P., García, H. E., Locarnini, R. A., Baranova, O. K., Bouchard, C., et al. (2023). World Ocean Atlas 2023. (nutrients and oxygen) [Dataset]. *NOAA National Centers for Environmental Information*. https://doi.org/10.25921/va26-hv25

Reyes−Mendoza, O., Manta, G., & Carrillo, L. (2022). Marine heatwaves and marine cold-spells on the Yucatan Shelf-break upwelling region. *Continental Shelf Research*, *239*, 104707. https://doi.org/10.1016/j.csr.2022.104707

Robson, J., Ortega, P., & Sutton, R. (2016). A reversal of climatic trends in the North Atlantic since 2005. *Nature Geoscience*, *9*(7), 513–517. https://doi.org/10.1038/ngeo2727

Sanders, R. N. C., Jones, D. C., Josey, S. A., Sinha, B., & Forget, G. (2022). Causes of the 2015 North Atlantic cold anomaly in a global state estimate. *Ocean Science*, *18*(4), 953–978. https://doi.org/10.5194/os-18-953-2022

Scannell, H. A., Johnson, G. C., Thompson, L., Lyman, J. M., & Riser, S. C. (2020). Subsurface evolution and persistence of marine heatwaves in the Northeast Pacific. *Geophysical Research Letters*, *47*(23), e2020GL090548. https://doi.org/10.1029/2020GL090548

Schlegel, R., Darmaraki, W. S., Benthuysen, J. A., Filbee-Dexter, K., & Oliver, E. C. J. (2021). Marine cold-spells. *Progress in Oceanography*, *198*, 102684. https://doi.org/10.1016/j.pocean.2021.102684

Schlegel, R. W., Oliver, E. C. J., Wernberg, T., & Smit, A. J. (2017). Nearshore and offshore co-occurrence of marine heatwaves and cold-spells. *Progress in Oceanography*, *151*, 189–205. https://doi.org/10.1016/j.pocean.2017.01.004

Shi, J., Wang, J., Ren, Z., Tang, C., & Huang, F. (2023). Cold blobs in the subpolar North Atlantic: Seasonality, spatial pattern, and driving mechanisms. *Ocean Dynamics*, *73*(5), 267–278. https://doi.org/10.1007/s10236-023-01553-z

Siddiqui, A. H., Haine, T. W. N., Nguyen, A. T., & Buckley, M. W. (2024). Controls on upper ocean salinity variability in the eastern subpolar North Atlantic during 1992–2017. *Journal of Geophysical Research: Oceans*, *129*(8), e2024JC020887. https://doi.org/10.1029/2024JC020887

Suryan, R. M., Arimitsu, M. L., Coletti, H. A., Hopcroft, R. R., Lindeberg, M. R., Barbeaux, S. J., et al. (2021). Ecosystem response persists after a prolonged marine heatwave. *Scientific Reports*, *11*(1), 623.5. https://doi.org/10.1038/s41598-021-83818-5

Thomas, A., Ramkumar, A., & Shanmugam, A. (2021). CO2 acidification and its differential responses on aquatic biota – A review. *Environmental Advances*, *8*, 100219. https://doi.org/10.1016/j.envadv.2022.100219

Wang, Y., Kajtar, J. B., Alexander, L. V., Pilo, G. S., & Holbrook, N. J. (2022). Understanding the changing nature of marine cold-spells. *Geophysical Research Letters*, *49*(6), e2021GL097002. https://doi.org/10.1029/2021GL097002

Wang, Y., & Zhou, y. (2024). Seasonal dynamics of global marine heatwaves over the last four decades. *Frontiers in Marine Science*, *11*. https://doi.org/10.3389/fmars.2024.1406416

Wheeler, P. A., Huyer, A., & Fleischbein, J. (2003). Cold halocline, increased nutrients and higher chlorophyll off Oregon in 2002. *Geophysical Research Letters*, *30*(15). https://doi.org/10.1029/2003gl017395

Yeager, S. G., Kim, W. M., & Robson, J. (2016). What caused the Atlantic cold blob of 2015. *US CLIVAR Variations*, *14*(2), 24–31.

Zapata, F. A., Jaramillo-Gonzalez, J., & Navas-Camacho, R. (2011). Extensive bleaching of the coral Porites lobata at Malpelo Island, Colombia, during a cold water episode in 2009. *Boletín de Investigaciones Marinas y Costeras-INVEMAR*, *40*, 185–193.

Zhang, C., Hu, C., Shang, S., Müller-Karger, F. E., Li, Y., Dai, M., et al. (2006). Bridging between SeaWiFS and MODIS for continuity of chlorophyll-a concentration assessments off Southeastern China. *Remote Sensing of Environment*, *102*(3–4), 250–263. https://doi.org/10.1016/j.rse.2006.02.015

Zhang, M., Li, L., Liu, Y., & Gao, X. (2019). Effects of a sudden drop in salinity on immune response mechanisms of Anadara kagoshimensis. *International Journal of Molecular Sciences*, *20*(18), 4365. https://doi.org/10.3390/ijms20184365